

ELEC 4700 Assignment - 2

Finite Difference Method

Submitted by: Chloe Ranahan (101120978)

1.

a) Simple Case with $V = V_0$ at $x = 0$ and $V = 0$ at $x = L$

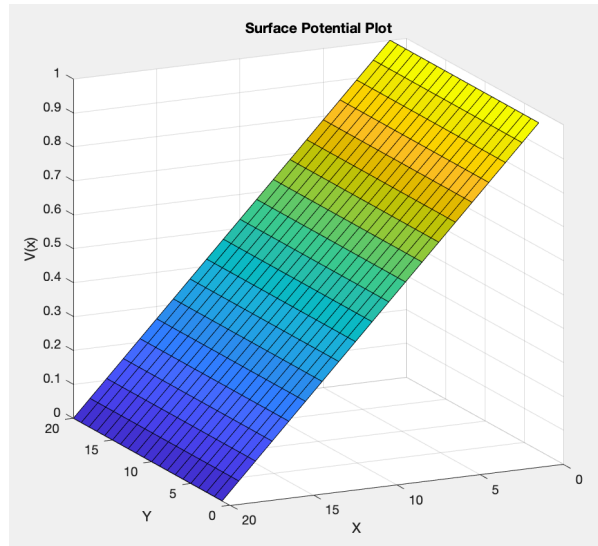


Figure 1: The surface potential plot for the case without fixed top or bottom boundary conditions ($V = V_0$ at $x = 0$ and $V = 0$ at $x = L$).

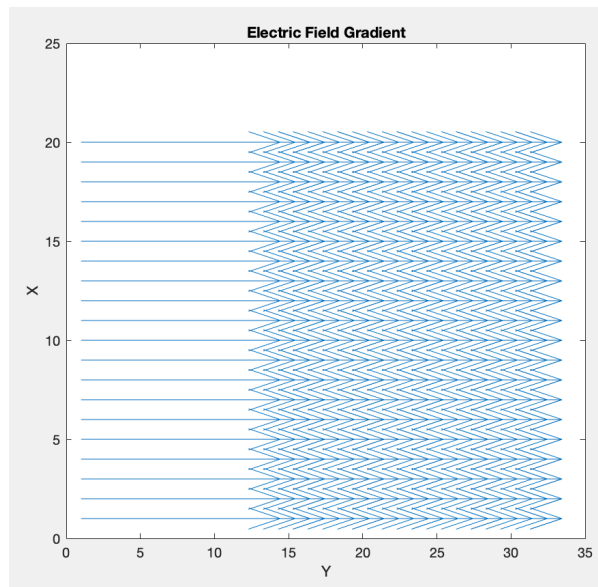


Figure 2: The electric field gradient for the case without fixed top or bottom boundary conditions ($V = V_0$ at $x = 0$ and $V = 0$ at $x = L$).

b) Case with $V = V_0$ at $x = 0, x = L$ and $V = 0$ at $y = 0, y = W$

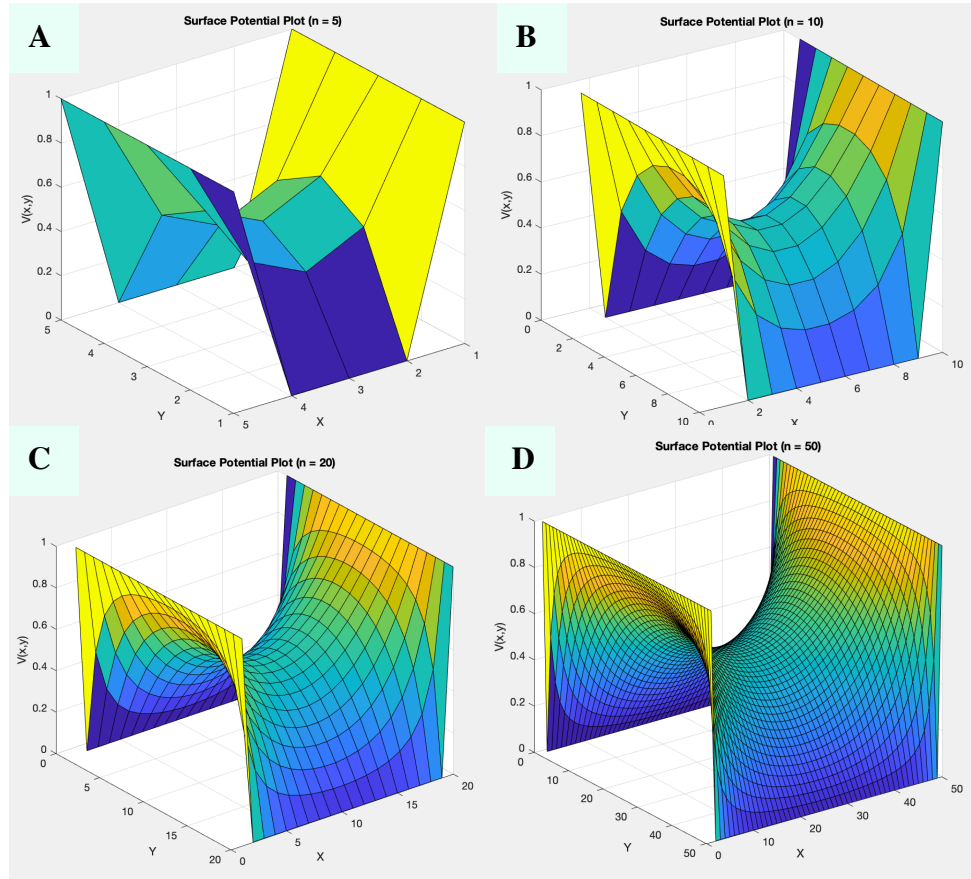


Figure 3: The surface potential plot for the case with fixed top and bottom boundary conditions ($V = V_0$ at $x = 0, x = L$ and $V = 0$ at $y = 0, y = W$). Mesh sizes for the solutions are: A) 5, B) 10, C) 20, D) 50.

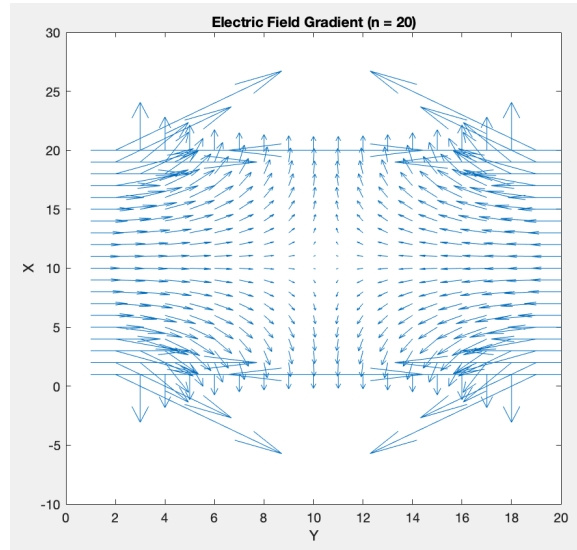


Figure 4: The electric field gradient for the case with fixed top and bottom boundary conditions, with a mesh size of 20.

Analytical Series Solution

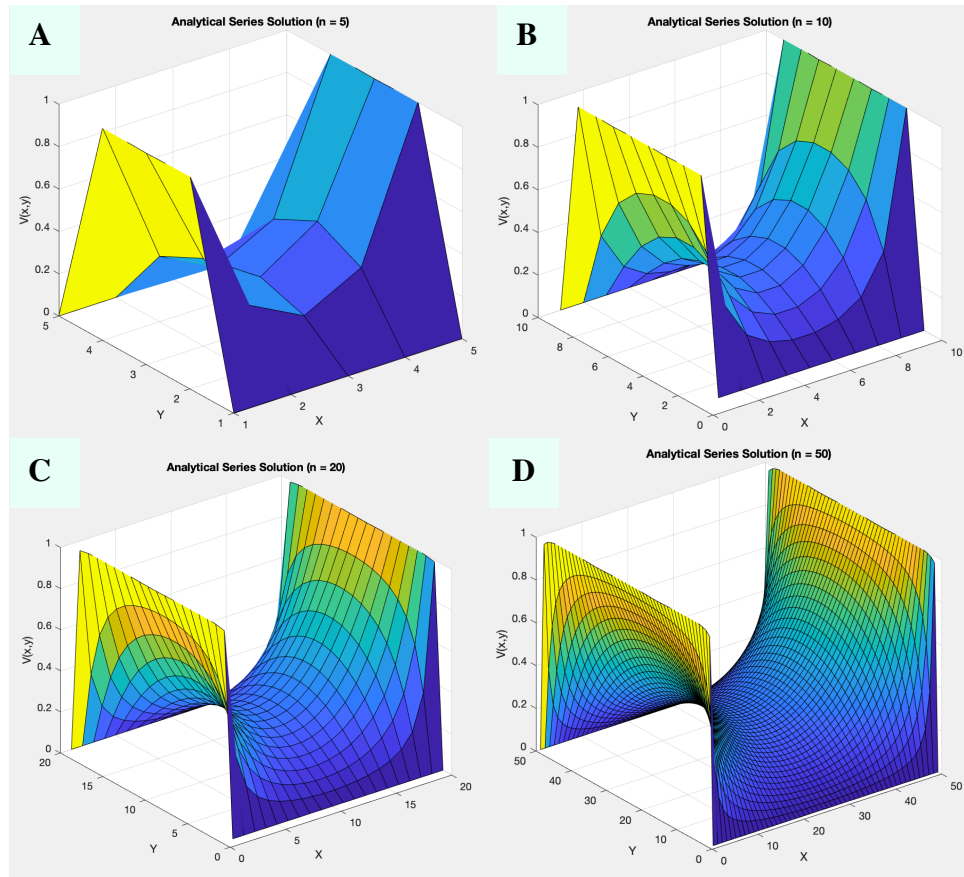


Figure 5: The surface potential plot for the analytical series solution to the case with fixed top or bottom boundary conditions ($V = V_0$ at $x = 0, x = L$ and $V = 0$ at $y = 0, y = W$). Mesh sizes for the solutions are: A) 5, B) 10, C) 20, D) 50.

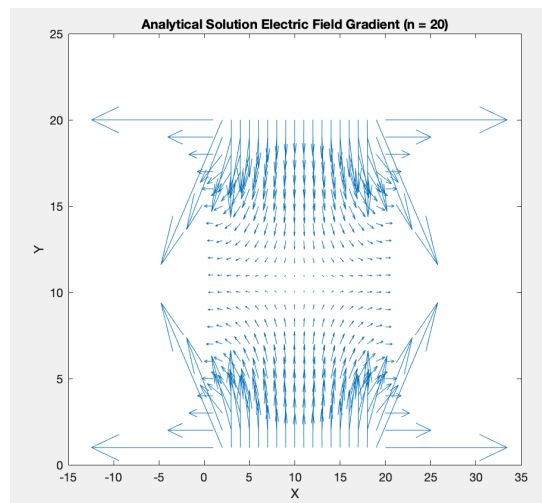


Figure 6: The electric field gradient for the analytical series solution to the case with fixed top and bottom boundary conditions, with a mesh size of 20.

Both the simple case a) and the case with boundary conditions b) were solved using a G matrix using the orthogonal resistor network model. In my codes' main for loops, the boundary conditions were defined (using $F(n)$), and the G matrix ($G(n, n)$) was defined as 1 when on the left or right edge of the rectangular region. For the top and bottom edges, $G(n, n)$ was defined as -3 so as to include the 3 connected "resistors" (adjacent currents). The centre region had $G(n, n)$ defined as -4 to include the 4 connected "resistors" (adjacent currents). The analytical solution was obtained using a series from $n = 1:300$, which was used as a representation of the infinite series solution described in the Griffiths text. As described in the Griffiths text, the constant 'a' was defined as the maximum y height (W) and the constant 'b' was defined as half of the total x width ($L/2$).

The simple case had insulated top and bottom conditions and gave a linear sloped solution (Figure 1), as expected. Figure 2 shows the electric field for this case, which was similarly linear and constant. Both the numerical and analytical solutions for the BC case had a saddle structure (Figure 3, 5), which became more evident at higher mesh sizes. Their electric field gradients were also found (Figure 4, 6), and were at a maximum at the corners, which was expected due to the boundary conditions of the adjacent edges being tied 0 (y) and V_0 (x).

As the mesh size for both the numerical (Figure 3) and analytical (Figure 5) solutions was increased, so did their similarity. Mesh sizes on the order of 100 and greater had significant simulation times, hence $n = 50$ was used as the maximum mesh size and was found to give the most accurate numerical solution (comparing to the analytical model).

The greatest discrepancy between the two methods was around the boundary conditions, and was more notable for smaller mesh sizes. The numerical solution for $n = 5$ (Figure 3A) had the x boundary conditions taking "priority", with V tied to V_0 at $x = 0$ and $x = L$. The y boundary conditions ($V = 0$ when $y = 0, W$) were only satisfied when x was not equal to 0 or L . The opposite was true for the analytical model for $n = 5$ (Figure 5A). The y boundary conditions had "priority", with V tied to 0 at $y = 0$ and $y = W$, whereas the x boundary conditions ($V = V_0$ when $x = 0, L$) were only satisfied when Y was not equal to 0 or W . However, with a mesh size of about $n = 20$ and above, these discrepancies became relatively small.

On top of the BC differences, the analytical solution appeared to have non-converged corners (Figure 5D), which could be fixed by making the sum closer to an infinite sum (the sum was done up to 300 in this case). This attribute of the analytical solution could be a good indicator of when to stop the series. Once the corners converge and start to resemble the numerical solution (Figure 3D), then the analytical series should be great enough to closely resemble the infinite solution.

The main advantages of using the analytical method is that it is not as limited by the discretization (not as limited by n_x , n_y), and that it doesn't require you to put in as much work to define the BCs. However, it does require the fully derived equation for the series solution you're modelling. Although the numerical solution requires precise BCs to be defined, it doesn't require the full derivation like the analytical solution. In addition, the numerical solution does not have the issue of non-converging corners like the analytical solution.

2.

a) Current Flow at the Two Contacts

The current at either edge ($x = 0$, n_x) was calculated by dividing the edges up into segments of W/n_y , then summing the current ($J(x)$ multiplied by Δy) at each point along y .

As expected, the total current at the left edge (SumIL) was equivalent to that at the right edge (SumIR). This current (for $n = 50$) was about 0.71 nA.

	SumIL	7.1002e-10
	SumIR	7.1002e-10

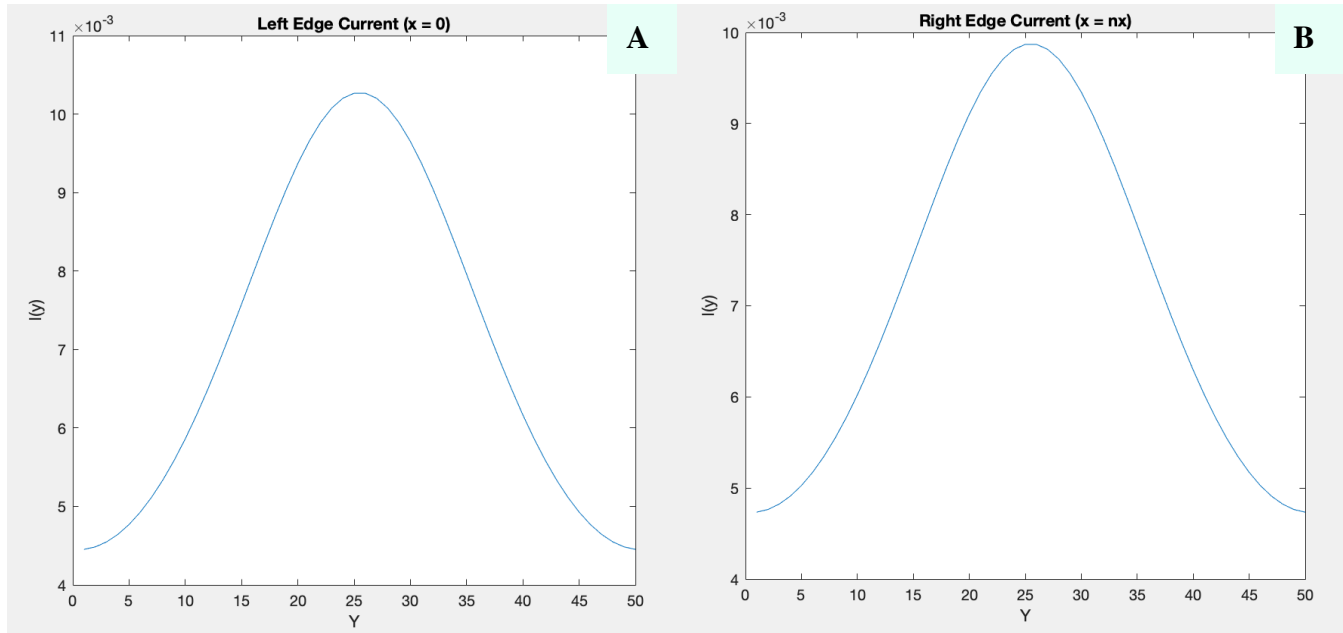


Figure 7: A) The left edge ($x = 0$) current along y , and B) the right edge ($x = n_x$) current along y .

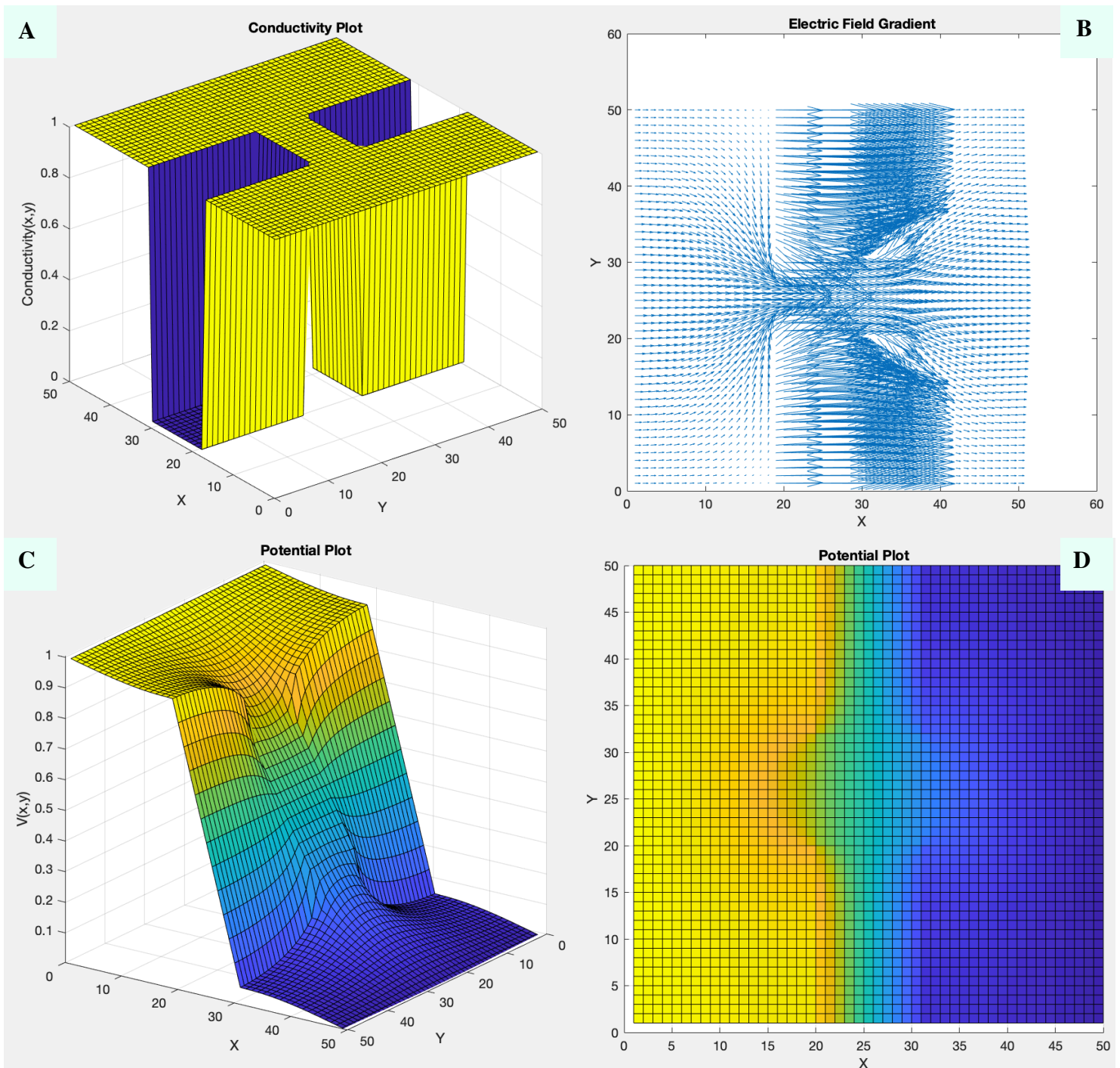


Figure 8: The conductivity $\sigma(x, y)$ (A), electric field gradient $E(x, y)$ (B), and potential $V(x, y)$ in a region with 2 rectangles of reduced conductivity. The potential is shown in 3D (C) and 2D (D).

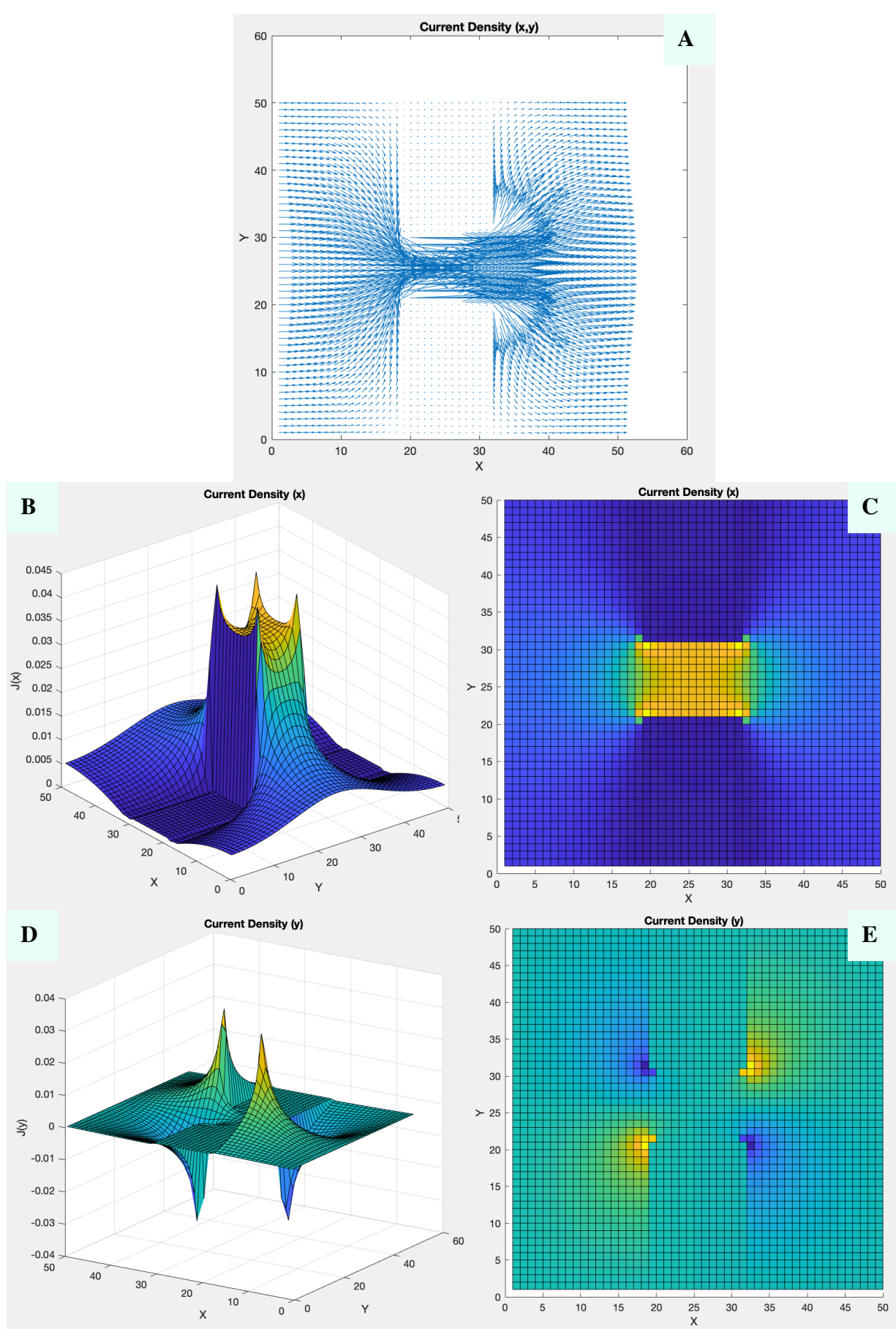


Figure 9: Current density (J) in a region with 2 rectangles of reduced conductivity. The total current density $J(x, y)$ (A), $J(x)$ shown in 3D (B) and 2D (C), $J(y)$ shown in 3D (D) and 2D (E).

The conductivity plot (Figure 8A) was exactly as expected. The conductivity outside the boxes was set to 1 and the conductivity within the boxes was set to 10^{-2} . Since electric field is inversely proportional to conductivity as shown by Ohm's Law ($J = \sigma E$), it makes sense that the electric field gradient is high at the region's bottleneck, and at a maximum through the low conductivity boxes (Figure 8B). The potential across the region drops off sharply across the boxes, but has a less steep downwards slope within the gap (Figure 8C, D) due to the higher current in that region. Current density was calculated by multiplying conductivity and electric field (i.e., $J_x = C \times E_x$). The current density was at a maximum within the gap (Figure 9A), which was expected due to the higher conductivity within that region relative to the boxes above and below it. Figure 9B, C show the current density in the x direction across the region. The greatest current density flowing across the rectangle in the x direction was found in the gap and at the corners of the boxes for the same reasons as explained before. Figure 9D, E show the current density in the y direction across the region. The maximum magnitude of current density flowing in the y direction was found at the corners of the boxes due to the bottleneck (current being squeezed through and then "overflowing" out). This phenomenon can also be seen by the arrows in the total current density plot (Figure 9A).

b) Investigating Mesh Density

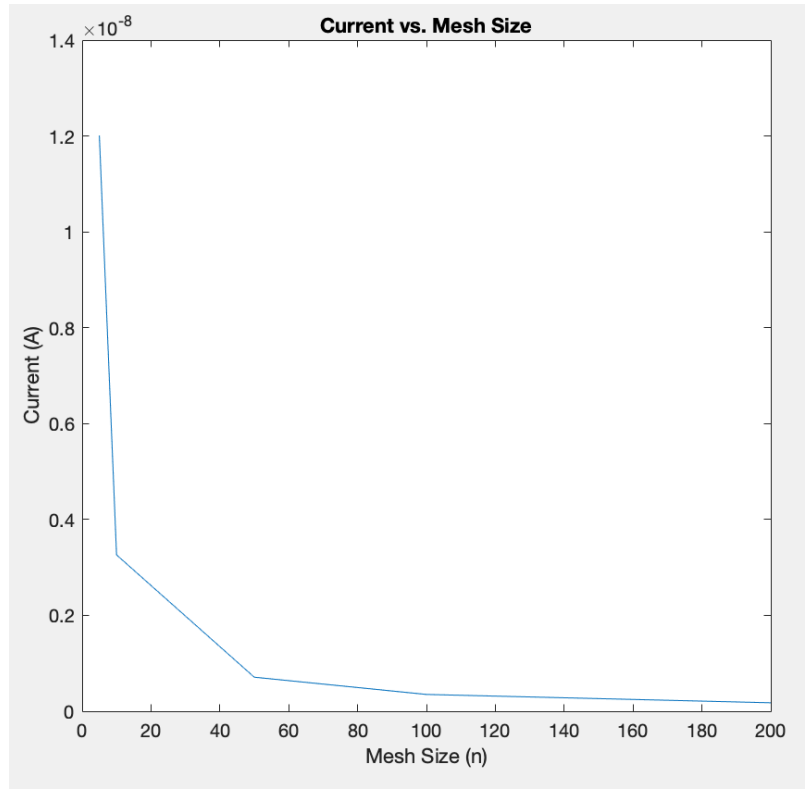


Figure 10: Graph of the relationship between current and mesh size (for mesh sizes of $n = 5, 10, 50, 100, 200$). The conductivity of the box was set to 10^{-2} and the bottleneck size to 0.2×10^{-7} m.

As seen in Figure 10, the current (left edge current was used) decreased exponentially as the mesh size was increased. As discussed in part 1, the accuracy of the numerical solution increased along with mesh size. Therefore, it appears that the edge currents were overestimated at small mesh sizes, then exponentially approach the correct edge current as the mesh size was increased.

c) Investigating Narrowing of the Bottleneck

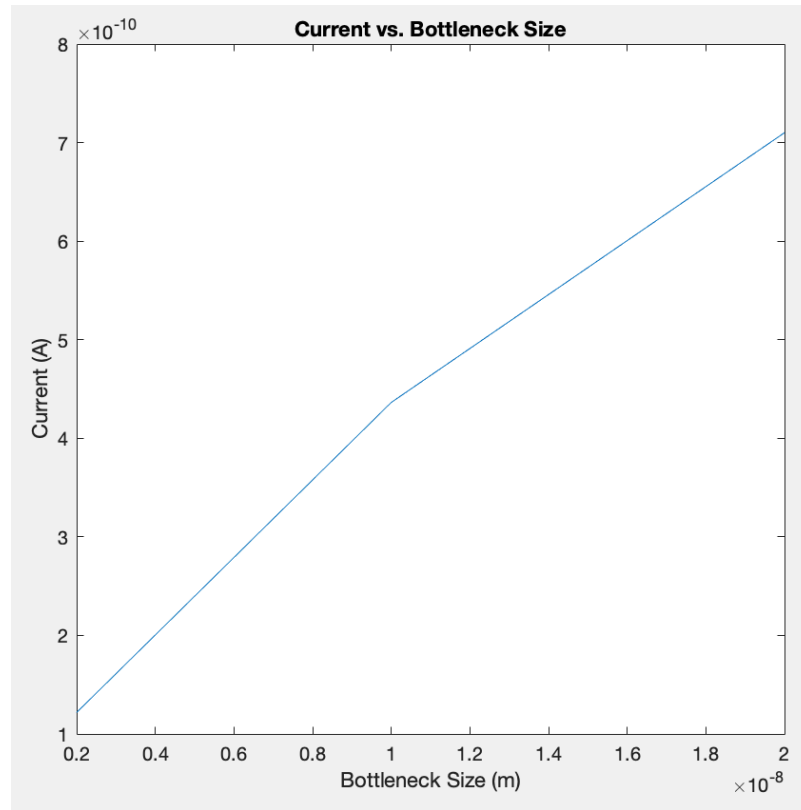


Figure 11: Graph of the relationship between current and bottleneck size (for bottleneck sizes of 2×10^{-8} m, 1×10^{-8} m and 0.2×10^{-8} m). The conductivity of the box was set to 10^{-2} and the mesh size to 50.

As shown above, the current was found to increase approximately linearly with bottleneck size. This positive relationship was expected since the boxes of lower conductivity have much lower currents throughout them. Therefore, minimizing the vertical (y) gap between the low conductivity boxes would limit the current flow able to pass through in the x direction.

d) Investigating Varying the Conductivity of the Boxes

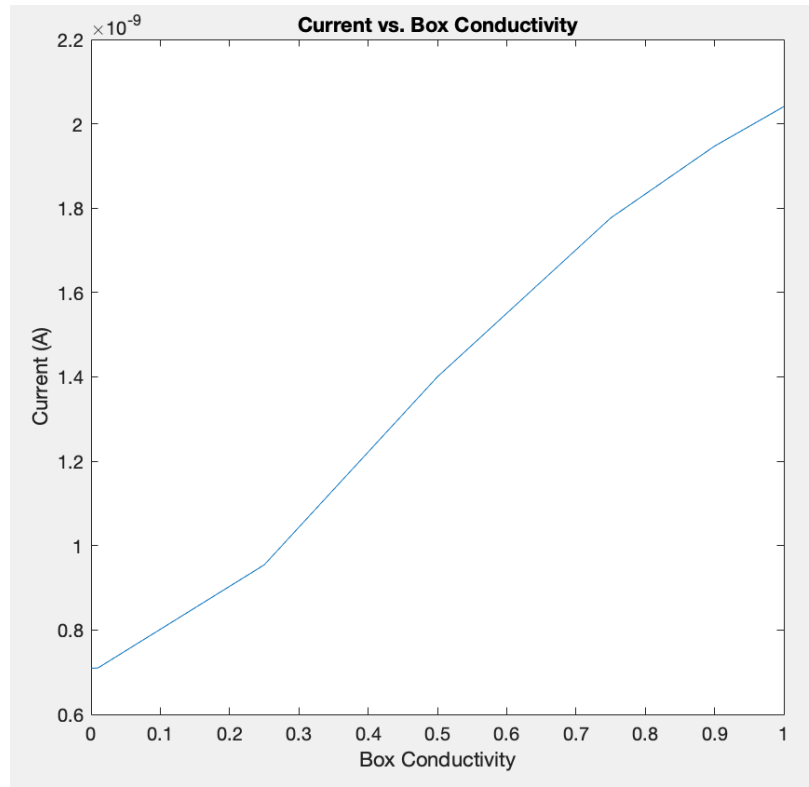


Figure 12: Graph of the relationship between current and box conductivity (for box conductivities of 1, 0.9, 0.75, 0.5, 0.25, 10^{-2} , 10^{-3} , and 10^{-4}). The bottleneck size was set to 0.2×10^{-7} m and the mesh size to 50.

As seen in Figure 12, the current roughly increases linearly along with the box conductivity. This makes sense since the current should be able to more readily pass through the boxes as their conductivities are increased up to that of the surrounding region (1). At a box conductivity of 1, there would no longer be a bottleneck observed as the current would flow with equivalent resistance inside and outside the boxes. On top of the current-box conductivity relationship, this graph can provide us with information on the minimum and maximum currents in the region. Since 1 is the maximum conductivity, the current for a box (& region) conductivity of 1 will give the maximum current (2.0408 nA). On the other hand, the currents for box conductivities of 10^{-3} , and 10^{-4} were very similar (0.70931 nA and 0.70928 nA, respectively), which demonstrates the lower limit of current for that box size. Decreasing the conductivity beyond those very small values doesn't impact the current too much since the vast majority of the current would be flowing through the bottleneck anyways.